SPANDIDOS PUBLICATIONS

ONCOLOGY REPORTS 49: 28, 2023

Anesthetic-specific lncRNA and mRNA profile changes in blood during colorectal cancer resection: A prospective, matched-case pilot study

ANJA LINDEMANN[1], FLORIAN BRANDES[2], MELANIE BORRMANN[2], AGNES S. MEIDERT[2], BENEDIKT KIRCHNER[3], ORTRUD K. STEINLEIN[1], GUSTAV SCHELLING[2], MICHAEL W. PFAFFL[3] and MARLENE REITHMAIR[1]

[1]Institute of Human Genetics, University Hospital, Ludwig-Maximilians-University Munich, 80336 Munich; [2]Department of Anesthesiology, University Hospital, LMU Munich, 81377 Munich; [3]Division of Animal Physiology and Immunology, School of Life Sciences Weihenstephan, Technical University of Munich, 85354 Freising, Germany

Received July 22, 2022; Accepted November 3, 2022

DOI: 10.3892/or.2022.8465

Abstract. Prometastatic and antitumor effects of different anesthetics have been previously analyzed in several studies with conflicting results. Thus, the underlying perioperative molecular mechanisms mediated by anesthetics potentially affecting tumor phenotype and metastasis remain unclear. It was hypothesized that anesthetic-specific long non-coding RNA (lncRNA) expression changes are induced in the blood circulation and play a crucial role in tumor outcome. In the present study, high-throughput sequencing and quantitative PCR were performed in order to identify lncRNA and mRNA expression changes affected by two therapeutic regimes, total intravenous anesthesia (TIVA) and volatile anesthetic gas (VAG) in patients undergoing colorectal cancer (CRC) resection. Total blood RNA was isolated prior to and following resection and characterized using RNA sequencing. mRNA-lncRNA interactions and their roles in cancer-related signaling of differentially expressed lncRNAs were identified using bioinformatics analyses. The comparison of these two time points revealed 35 differentially expressed lncRNAs in the TIVA-group, and 25 in the VAG-group, whereas eight were shared by both groups. Two lncRNAs in the TIVA-group, and 23 in the VAG-group of *in silico* identified target-mRNAs were confirmed as differentially regulated in the NGS dataset of the present study. Pathway analysis was performed and cancer relevant canonical pathways for TIVA were identified. Target-mRNA analysis of VAG revealed a markedly worsened immunological response against cancer. In this proof-of-concept study, anesthesic-specific expression changes in lncRNA and mRNA profiles in blood were successfully identified. Moreover, the data of the present study provide the first evidence that anesthesia-induced lncRNA pattern changes may contribute further in the observed differences in CRC outcome following tumor resection.

Correspondence to: Dr Marlene Reithmair, Institute of Human Genetics, University Hospital, Ludwig-Maximilians-University Munich, Goethestraße 29, 80336 Munich, Germany
E-mail: marlene.reithmair@med.uni-muenchen.de

Abbreviations: CRC, colorectal cancer; DGE, differential gene expression; FC, fold change; padj, adjusted P-value; PCA, principal component analysis; RT-qPCR, reverse transcription-quantitative polymerase chain reaction; TIVA, total intravenous anesthesia; VAG, volatile anesthetic gas; HIPK2, homeodomain interacting protein kinase 2; SPN, sialophorin; P2RX7, purinergic receptor P2X 7; ALDH5A1, aldehyde dehydrogenase 5 family member A1; lncRNA, long non-coding RNA

Key words: colorectal cancer, total intravenous anesthesia, volatile anesthetic gas, lncRNA, target-mRNA, signaling pathways

Introduction

Colorectal cancer (CRC) remains the third leading cause of cancer-related mortality worldwide regardless of the availability of improved diagnostic and therapeutic strategies (1). Surgical resection in combination with radiotherapy and chemotherapy, depending on cancer stage, offers the best chances of survival for patients and represents the standard of clinical care (2). Removal of the primary tumor carries a risk of subsequent metastatic tumor spread, due to the potential release of tumor cells into the circulation. In addition, surgical trauma to adjacent healthy tissues can support metastasis, since neoangiogenesis increases during wound healing (3,4). Perioperative factors such as the choice of anesthesia may have an influence on carcinogenesis, metastasis, recurrence, and the final clinical outcome; however these effects have not been fully elucidated (5,6). Surgery for CRC is performed under general anesthesia. For the maintenance of anesthesia, two anesthetics are most commonly used: Either total intravenous anesthesia (TIVA) using propofol, or a volatile anesthetic gas (VAG), with sevoflurane being the mostly commonly administered. For TIVA, a reduced intraoperative inflammatory

reaction has been observed in several studies (7-9). In a retrospective study on CRC patients who received propofol or desflurane (another VAG), the use of propofol led to a significantly longer and higher overall survival with reduced metastasis occurrence (10-13). However, the mechanisms underlying these observations remain largely unknown. In contrast to TIVA, studies investigating VAG in this context have demonstrated no consistent trend concerning tumor cell growth, metastasis or protective effects (11,14-17). Recently, the identification of regulatory non-coding RNAs, including microRNAs (miRNAs/miRs) and long non-coding RNAs (lncRNAs), has increased the complexity of the molecular landscape (18,19).

Numerous investigations have characterized the important function of miRNAs in tumor biology. A recent study by the authors demonstrated anesthetic-specific effects on expression levels of miRNAs co-precipitating with extracellular vesicles when the VAG sevoflurane was compared to TIVA. *In silico* target analyses of microRNA expression patterns in this study indicated an inhibitory effect of propofol on crucial carcinoma-related pathways, including proliferation, migration and enhanced apoptosis (19). In contrast to the well-established role of miRNAs, lncRNAs and their impact on cancer is a relatively new research field, both being specifiable on their size and function. LncRNAs are not translated, consist of minimum 200 nucleotides up to kilobases (20-22) and have been attributed important functions in transcription, translation and post-translational modification (23,24). In the field of tumor biology, lncRNAs can either inhibit tumor growth or act as oncogenes, promoting cell proliferation and migration (25-27); however, the potential effect of anesthetic agents on lncRNAs has not been investigated previously, to the best of our knowledge.

The hypothesis that the present study was based on is that anesthetic-specific lncRNA expression changes are induced in the blood circulation and may play a crucial role in tumor outcome.

The primary aim of the present study was to perform a proof-of-concept study, in order to demonstrate the differential effects of TIVA (propofol) on blood-derived lncRNA and mRNA profiles, in comparison to VAG (sevoflurane), during CRC resection. Secondly, the present study was designed to provide preliminary evidence of cancer relevant signaling changes induced by lncRNA-mRNA regulatory effects. It was designed as a prospective, matched-case, non-randomized pilot study, including patients undergoing colorectal cancer surgery at the LMU Hospital Munich, anesthetized with TIVA or VAG and fulfilling the predefined inclusion criteria. To obtain holistic lncRNA and mRNA expression profiles, a high-throughput sequencing approach with subsequent quantitative PCR confirmation was applied. Differential gene expression (DGE) analysis of mRNA and lncRNA sequencing data permitted the validation of *in silico* identified target-mRNAs and to confirm significant changes in target-mRNA expression. Consequently, it was feasible to identify differentially regulated lncRNAs, which possibly modulate target-mRNAs and play a crucial role in cancer relevant signaling pathways. This type of differentially expressed and anesthetic-specific lncRNAs and their identified target-mRNAs represent candidates for the still unexplained mechanism that may influence long-term survival of cancer patients following the surgical removal of the tumor.

Materials and methods

Patient identification and selection. Patient recruitment and matching were performed as previously described (19). The Ethics Committee of the Medical Faculty of the Ludwig-Maximilians-University (LMU) Munich, Germany (to which the Institute of Human Genetics and the Department of Anesthesiology are assigned) approved the present study (protocol-no. 232-16). The present study was performed in accordance with the Declaration of Helsinki. Written informed consent was obtained and study samples were pseudonymized. Inclusion and exclusion criteria were applied for both the TIVA and VAG group. The inclusion criteria were the presence of a primary colorectal cancer scheduled for operative therapy and consent to the study. The exclusion criteria were the following: i) Denied consent; ii) an age <18 years; iii) pregnancy; iv) the simultaneous occurrence of CRC with another primary tumor; v) severe organ dysfunction (liver, kidney); vi) chronic inflammatory or autoimmune disorder (e.g., rheumatoid arthritis); vii) the use of immunosuppressive medication; and viii) contraindications for epidural anesthesia. The final study cohort consisted of 12 patients receiving TIVA and 10 patients receiving VAG. All patients underwent open surgery procedure for CRC resection and were recruited at the University Hospital of Munich from 04/2017 to 06/2018. Statistical power calculation for sample size assessment was not performed, since to the best of our knowledge there are no studies available dealing with the effect of anesthetic agents on blood-derived lncRNA expression profiles. The patient cohorts were comparable with regard to demographic variables, comorbidities and perioperatively administered medication. The mean age was 71.90 years with a standard deviation (SD) of 10.13 years for the VAG group, and 61.58 years with a SD of 10.95 years for the TIVA group. The sex distribution was 7 males/5 females in the TIVA group, and 8 males/2 females in the VAG group. In particular, the cohorts did not differ significantly in the primary matching goals of tumor stage (P=0.162) and localization (P=0.595) (Table I).

Anesthesiologic procedures and sample collection. Standard balanced anesthesia consisting of an epidural in combination with general anesthesia was planned for all patients. For 3 patients, epidural anesthesia was not possible. due to anatomical reasons. General anesthesia was induced with propofol in both groups and subsequently maintained with propofol (TIVA) or sevoflurane (VAG).

A maximum of 44.2 ml of blood was collected per patient. Venous blood was drawn through intravascular catheters at the preoperative time point and after termination of surgery during wound closure (post-operative time point). For collection and stabilization of the 2.5 ml whole blood samples, RNA tubes (PAXgene; Qiagen GmbH; cat. no. 762165) were used according to the manufacturer's protocol and stored at -80˚C until further processing.

RNA extraction, depletion, library preparation and sequencing. Total blood RNA containing the red and the white

Table I. Overview of the patient characteristics divided according to the anesthetic agent used.

Parameter	TIVA	VAG	P-value
Sex			
Male	7	8	0.531
Female	5	2	
Age in years[a] (age range)	59.5 (54.8-66.0)	71.0 (66.2-80.8)	0.016
BMI (kg/m^2)[a]	25.1 (21.3-26.9)	26.7 (24.1-36.6)	0.069
ASA classification[b] (3/2)			
3	10	9	0.865
2	2	1	
Tumor location			
Rectal	6	7	0.595
Right colon	3	3	
Left colon	1	0	
Sigmoid	2	0	
UICC stage[c]			0.162
I	1	3	
II	3	2	
III	8	3	
IV	0	2	
Coronary heart disease			
No	12	7	0.156
Yes	0	3	
Arterial hypertension			
No	8	4	0.412
Yes	4	6	
Diabetes			
No	12	6	0.062
Yes	0	4	
Kidney insufficiency			
No	12	9	0.926
Yes	0	1	
Atrial fibrillation			
No	12	7	0.156
Yes	0	3	
Preoperative radiation			
No	7	5	0.969
Yes	5	5	
Preoperative chemotherapy			
No	7	7	0.903
Yes	5	3	
Epidural anesthesia			
No	2	1	0.865
Yes	10	9	
Duration of anesthesia, in min; value (range)[a]	390.0 (286.2-545.5)	337.5 (313.2-418.8)	0.5
Maximum dosage of noradrenaline in mg/h; value (range)[a]	0.4 (0.3-0.6)	0.6 (0.5-1.0)	0.016
Maximum MAC; value (range)[a,d]	0.0 (0.0-0.0)	1.2 (1.0-1.4)	<0.001
Fluids (liters)[a]	3.5 (3.0-5.25)	4.25 (3.63-4.9)	0.264
Duration of surgery, in min; value (range)[a]	282.5 (191.8-403.0)	234.0 (204.2-291.8)	0.288
Cumulative dosage of ropivacaine[d] in mg; value (range)[a]	190.0 (155.0-241.2)	165.0 (152.5-180.0)	0.113
Cumulative dosage of propofol during anesthesia in mg/kg of body weight (value range)[a]	32.0 (23.5-44.9)	5.6 (1.7-7.6)	<0.001
Cumulative dosage of sufentanil in mg/kg of body weight; value (range)[a]	1.0 (0.6-1.2)	0.9 (0.7-1.0)	0.334

[a]Data are the median (25-75% quartile); [b]ASA physical status classification system; [c]Union for International Cancer Control, 8th edition 2017 (79); [d]Administered in the epidural catheter. TIVA, total intravenous anesthesia; VAG, volatile anesthetic gas; BMI, body mass index; ASA, American Society of Anesthesiologists; UICC, Union for International Cancer Control; MAC, minimum alveolar concentration.

blood cell fraction (ratios of lymphocytes and macrophages as physiologically present in human blood) was extracted using the PAXgene system with the PAXgene blood miRNA kit (Qiagen GmbH; cat. no. 763134). To achieve higher concentrations, the samples were evaporated and eluted in a smaller volume of 28 μl. The integrity of total blood cell derived RNA was assessed using capillary electrophoresis, using the RNA 6000 Nano kit (Agilent Technologies GmbH; cat. no. 5067-1511) on the Bioanalyzer 2100 (Agilent Technologies GmbH). To remove highly abundant RNA like cytoplasmic and mitochondrial rRNA and globin mRNA the QIAseq® FastSelect -rRNA/Globin kit (Qiagen GmbH; cat. no. 335376) was utilized. QIAseq™ Stranded Total RNA Library kit (Qiagen GmbH; cat. no. 180743) was used to generate RNA sequencing libraries from 800 ng total RNA input. Due to a moderate sample quality an insert size of ~150-250 bp was generated by a ten-minute incubation at 95˚C. To assess the size distribution and concentration of final libraries the High Sensitivity DNA kit (Agilent Technologies GmbH; cat. no. 5067-4626) on Bioanalyzer 2100 (Agilent Technologies GmbH) was performed. All kit protocols were applied according to the manufacturer's instructions. Samples were divided into four sequencing runs-two runs with 12 samples each and two with 10 samples each. In total, 50 cycles of single-end sequencing on the HiSeq2500 (Illumina GmbH) were performed, using the HiSeq Rapid SBS and SR Cluster kits (Illumina GmbH; Cat. nos. FC-402-4022 and GD-402-4002).

Bioinformatic RNA sequencing analysis. 3' adaptor sequences were excluded from the raw data sequences using Cutadapt (v2.8) (28) and reads with <16 nucleotides remaining were omitted. Trimmed reads were analyzed with the Fast QC software v.0.11.9 (https://www.bioinformatics.babraham.ac.uk/projects/fastqc/) to evaluate phred scores and read lengths before aligning them against the human genome (GRCh38) with STAR (v2.7.3a) (29). Aligned reads were then annotated using RSEM (v1.3.1) (30), to count reads mapping to coding sequences.

All samples were included for subsequent DGE analyses. DGE analyses for the identification of differentially expressed genes between the two time points, preoperatively and after the termination of the surgery during wound closure (postoperative) within each anesthetic group and between the TIVA- and VAG-groups, were performed using DESeq2 (v1.30.1) (31). Technical variation introduced by multiple sequencing runs was accounted for in the model. Benjamini-Hochberg method controlling the false discovery rate was applied to reduce type I error accumulation.

For lncRNA and mRNA analysis, transcripts that fulfilled the following filter criteria were selected: i) Mean expression (BaseMean) ≥50 normalized reads; ii) absolute value of $\log_2$ fold change ($|\log_2 FC|$) ≥1 for lncRNA, respectively $|\log_2 FC|$ ≥0.5 for mRNA transcripts; and iii) an adjusted P-value (padj) ≤0.1.

Target and pathway analysis. Using the software tool RNAInter v.4.0, target-mRNAs of significantly regulated lncRNAs were identified (32). Filter criteria for RNAInter were set to interaction type 'RNA-RNA interactions', species 'Homo sapiens' and a confidence score >0.5. The resulting target-mRNAs were compared with the mRNA DGE data. For lncRNAs without results (n=18 VAG, n=29 TIVA) in RNAInter, target-mRNAs were identified using a lncRNA identification and functional annotation tool called LncADeep v.1.0 (33), which among others identified the interaction with Kyoto Encyclopedia of Genes and Genomes (KEGG) pathways (34). However, only few pathways were unique (n=1 for VAG, n=14 for TIVA) and had no clinical relevance for CRC or anesthesia-related effects (Table SI). Ingenuity Pathway Analysis (IPA® version 81348237, Qiagen Digital Insights, a subsidary of Qiagen Inc.) was used for *in silico* analysis. Target-mRNAs were entered into IPA®, and only experimentally confirmed relationships were considered for signaling pathways identification and regulatory effect characterization.

Reverse transcription-quantitative polymerase chain reaction (RT-qPCR) validation. A technical validation via RT-qPCR (StepOnePlus™ Real-Time PCR System; Applied Biosystems™; Thermo Fisher Scientific, Inc.) was performed from the same RNA sample utilized for RNA sequencing libraries. A total RNA quantity of 400 ng was used for reverse transcription, applying the QuantiTect Reverse Transcription kit (Qiagen GmbH; Cat. no. 205313). The resulting cDNA was diluted 1:20 for RT-qPCR using the SsoAdvanced Universal SYBR-Green Supermix Kit (Bio-Rad Laboratories GmbH; Cat. no. 175272) and PrimePCR (lncRNA) SYBR-Green Assays (Bio-Rad Laboratories GmbH). Additionally, QuantiNova LNA PCR Assays for lncRNAs, HELLPAR_2464189 and TSIX_1589209 (Qiagen GmbH) and QuantiTect Primer Assay for lncRNA CCDC26 (https://geneglobe.qiagen.com/) were used for repeating the lncRNA HELLPAR, TSIX and CCDC26 quantification (Table II). Stable reference gene candidates to normalize relative gene expression levels were selected from RNA sequencing data utilizing the software tools geNorm and NormFinder (NormqPCR v1.44.0) (35-37). geNorm determines expression stability by assessing the pairwise variation as the standard deviation of the logarithmically transformed expression ratios of a particular gene to all other genes (termed gene-stability measure M). Lower M values indicate a more stable expression and genes with higher M values are iteratively discarded to reevaluate the remaining genes to find well suited references for normalization. Similarly, NormFinder estimates variances on logarithmically transformed measured gene expression to define a stability value for each gene, additionally attempting to minimize the estimated intra- and inter-group variation as well in a model-based approach. ZNF207, CAPZB and CORO1A were identified as reference candidates for the TIVA cohort among the top 15 in both tools with an M value threshold <0.5, and VIM, VMP1, RASSF2 and DENND3 as reference candidates for the VAG cohort (mean M value over all genes for TIVA 0.76 and for VAG 0.83). The RT-qPCR cycling conditions were as follows: 2 min at 95˚C once for activation, followed by 40 cycles of 5 sec at 95˚C and 30 sec at 60˚C. Melt curve steps were 65˚C to 95˚C at 0.5˚C increments for 5 sec/step. Following RT-qPCR, data were normalized with the geometric mean of the selected stable reference genes (ZNF207, CORO1A for the TIVA cohort, and VIM, VMP1, RASSF2, DENND3 for the VAG cohort. Relative quantification was performed applying the $2^{-\Delta\Delta Cq}$ method (38).

Table II. RT-qPCR validation of selected lncRNAs and mRNAs.

		RT-qPCR		RNA sequencing				
Group	Gene name	log_2FC	P-value	log_2FC	padj	Regulation	Primer assay ID	URL
TIVA	FAM157A[a]	1.041	0.02	-1.001	1.39E-02	Upregulated at the postoperative timepoint	qHsaCID0037478[d]	https://commerce.bio-rad.com/de-de/prime-pcr-assays/assay/qhsacid0037478-primepcr-sybr-green-assay-fam157a-human
	ST20-AS1[a]	0.778	0.05	-1.047	5.36E-02	Upregulated at the postoperative timepoint	qhsaLED0104269[d]	https://commerce.bio-rad.com/de-de/prime-pcr-assays/assay/qhsaled0104269-primepcr-sybr-green-assay-st20-as1-human
	HIPK2[b]	0.327	0.42	-0.780	4.21E-02	Upregulated at the postoperative timepoint	qHsaCID0016497[d]	https://commerce.bio-rad.com/de-de/prime-pcr-assays/assay/qhsacid0016497-primepcr-sybr-green-assay-hipk2-human
	BCL9L	No results No amplification		0.805	5.85E-02	Upregulated at the postoperative timepoint	qHsaCED0047806[d]	https://commerce.bio-rad.com/de-de/prime-pcr-assays/assay/qhsaced0047806-primepcr-sybr-green-assay-bcl9l-human
VAG	HELLPAR	No amplification		-1.234	3.26E-02	Upregulated at the postoperative timepoint	HS_HELLPAR_2464189[c] (Geneglobe ID SBH1217879); qhsaLED0090528[d]	https://geneglobe.qiagen.com/us/search?cat=&q=SBH1217879 https://commerce.bio-rad.com/de-de/prime-pcr-assays/assay/qhsaled0090528-primepcr-sybr-green-assay-hellpar-human
	CCDC26[c]	No amplification		-1.432	4.52E-02	Upregulated at the postoperative timepoint	HS_CCDC26_2SG[e] (Geneglobe ID QT02503214); qhsaLID0060379[d]	https://geneglobe.qiagen.com/us/search?cat=&q=QT02503214 https://commerce.bio-rad.com/de-de/prime-pcr-assays/assay/qhsalid0060379-primepcr-sybr-green-assay-ccdc26-human
	TSIX	No amplification		-1.419	3.10E-02	Upregulated at the postoperative timepoint	HS_TSIX_1589209[c] (Geneglobe ID SBH0345405); qhsaLED0059473[d]	https://geneglobe.qiagen.com/us/search?cat=&q=SBH0345405 https://commerce.bio-rad.com/de-de/prime-pcr-assays/assay/qhsaled0059473-primepcr-sybr-green-assay-tsix-human
	BCL2[a]	-1.826	<0.01	1.151	1.10E-06	Downregulated at the postoperative timepoint	qHsaCED0057245[d]	https://commerce.bio-rad.com/de-de/prime-pcr-assays/assay/qhsaced0057245-primepcr-sybr-green-assay-bcl2-human
	SPN/CD43[a]	-1.344	0.03	0.671	2.44E-02	Downregulated at the postoperative timepoint	qHsaCED0002014[d]	https://commerce.bio-rad.com/de-de/prime-pcr-assays/assay/qhsaced0002014-primepcr-sybr-green-assay-spn-human
	P2RX7/P2X7[a]	-1.078	0.01	0.807	4.69E-02	Downregulated at the postoperative timepoint	qHsaCID0012839[d]	https://commerce.bio-rad.com/de-de/prime-pcr-assays/assay/qhsacid0012839-primepcr-sybr-green-assay-p2rx7-human

Table II. Continued.

Group	Gene name	RT-qPCR		RNA sequencing			Primer assay ID	URL
		log_2FC	P-value	log_2FC	padj	Regulation		
Reference genes	ZNF207						qHsaCED0037802[d]	https://commerce.bio-rad.com/de-de/prime-pcr-assays/assay/qhsaced0037802-primepcr-sybr-green-assay-znf207-human
	CORO1A						qHsaCID0014041[d]	https://commerce.bio-rad.com/de-de/prime-pcr-assays/assay/qhsacid0014041-primepcr-sybr-green-assay-coro1a-human
	VIM						qHsaCID0012604[d]	https://commerce.bio-rad.com/de-de/prime-pcr-assays/assay/qhsacid0012604-primepcr-sybr-green-assay-vim-human
	VMP1						qHsaCID0016198[d]	https://commerce.bio-rad.com/de-de/prime-pcr-assays/assay/qhsacid0016198-primepcr-sybr-green-assay-vmp1-human
	RASSF2						qHsaCID0015249[d]	https://commerce.bio-rad.com/de-de/prime-pcr-assays/assay/qhsacid0015249-primepcr-sybr-green-assay-rassf2-human
	DENND3						qHsaCED0005069[d]	https://commerce.bio-rad.com/de-de/prime-pcr-assays/assay/qhsaced0005069-primepcr-sybr-green-assay-dennd3-human

[a]Confirmed using RT-qPCR; [b]not confirmed using RT-qPCR; [c]QuantiNova Assay by Qiagen, Inc.; [d]PrimePCR Assays by Bio-Rad Laboratories, Inc.; [e]QuantiTect Assay by Qiagen, Inc.; positive log_2FC in RT-qPCR means a lower Cq value at the postoperative time point than at the preoperative time point and thus an upregulation; positive log_2FC in RNA sequencing indicate downregulation; TIVA data were normalized with ZNF207 and CORO1A, VAG data with VIM, VMP1, RASSF2 and DENND3. RT-qPCR, reverse transcription-quantitative polymerase chain reaction; lncRNA, long non-coding RNA; padj, adjusted P-value; TIVA, total intravenous anesthesia; VAG, volatile anesthetic gas.

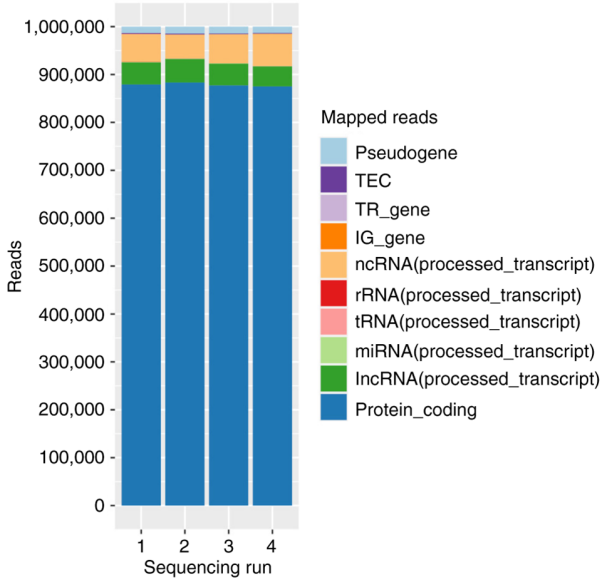

Figure 1. Mean annotation distribution for each of four sequencing runs. Within a run, both time points of patients from the TIVA and VAG groups were included. TIVA, total intravenous anesthesia; VAG, volatile anesthetic gas; RPM, reads per million; miRNA, micro RNA; tRNA, transfer-RNA, rRNA, ribosomal RNA, ncRNA, non-coding RNA, IG_gene, immunoglobulins_gene; TR_gene, thyroid hormone receptor_gene; TEC, tyrosine-protein kinase.

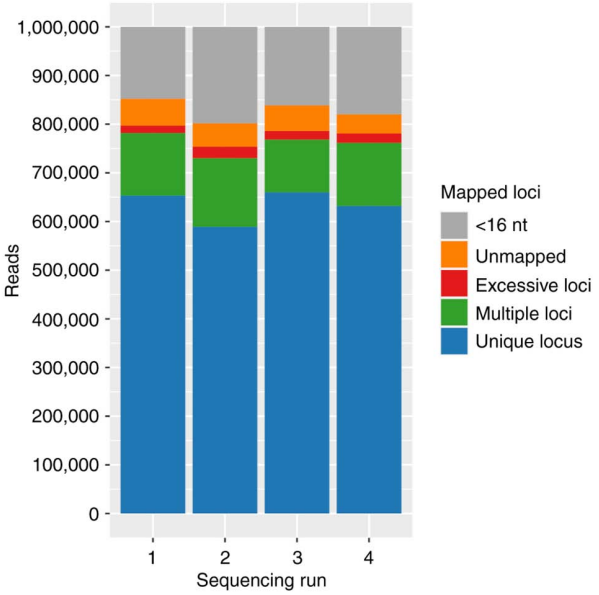

Figure 2. Mean mapping distribution for each of the four sequencing runs. Within a run, both time points of patients from the TIVA and VAG groups were included. TIVA, total intravenous anesthesia; VAG, volatile anesthetic gas.

Statistical analysis. Comparison of patients' demographical data and clinical parameters were performed with the non-parametic Mann-Whitney U test. Fisher's exact test was performed for two categorical variables, tumor location and stage according to Union for International Cancer Control (UICC). The Chi-squared test was performed for all other categorical variables. Differential gene expression data was corrected for false discovery according to the Benjamini-Hochberg correction (padj). IPA® (version 60467501; Qiagen, Inc.) was used for statistical data analyses. A P-value (adjusted P-value for NGS data) ≤0.1 was considered to indicate a statistically significant difference.

Results

RNA extraction and sequencing quality and quantity. The RNA integrity number of the extracted RNA determined by bioanalyzer was 8.033±1.333. Sequencing-quality control was performed using Fast QC software. Sequencing libraries of the runs were reasonably homogenous in size and composition (Figs. 1 and 2, and Table III). Run 1 and run 2 contained two VAG and three TIVA patients, and run 3 and run 4 contained 3 patients each.

Anesthesia-induced changes in lncRNA profiles. An intra-group comparison (paired analysis) was performed. DGE analysis considered the two time points within each of the two groups. In total, 35 differentially regulated lncRNAs in the TIVA-group (all upregulated) and 25 in the VAG-group (24 upregulated, one downregulated) were identified. A total of eight lncRNAs (RP6-159A1.4, MIR646HG, LINC00694, ST3GAL4-AS1, LINC00937, CTB-131B5.2, PLBD1-AS1, AC091878.1) were upregulated in both groups (Table IV). Several of these lncRNAs have already been shown to be associated with cancer: PLBD1-AS1 (39), TTN-AS1 (40-42), LINC01001 (43), RP11-701P16.5 (44), CTB-31N19.3/METTL9 (45), ST20-AS1 (46), HELLPAR (47), CCDC26 (48-50), LINC00511 (51-53), SNHG23 (MEG8) (54), TSIX (55), LINC01127 (56).

Anesthesia-induced changes in mRNA profiles. In addition to lncRNAs, DGE analysis of mRNAs between the pre- and postoperative time points revealed 1595 mRNAs in the TIVA-group and 947 in the VAG-group, respectively. Of these, 1047 mRNAs (TIVA) and 399 mRNAs (VAG) were agent-specific (Table SII).

In silico identification of lncRNA-associated target-mRNAs. Overall, 16 possible target-mRNAs were identified in relation to six lncRNAs in the TIVA-group. Concerning seven lncRNA from the VAG-group, 252 target-mRNAs were related. HELLPAR targeted 207 mRNAs, TSIX 36 and CCDC26 one, respectively. For 29 (TIVA) and 18 (VAG) lncRNAs, no target-mRNAs could be identified. The *in silico* identified target-mRNAs were compared with the mRNAs from the DGE analysis. In total, 12.5% (2 out of 16) of the *in silico* identified target-mRNAs for the TIVA-group, 9.13% (23 out of 252) for the VAG-group, respectively, satisfied the cut-off requirements for of the DGE analysis. Those remaining significantly regulated target mRNAs are presented in Table V and were subsequently analyzed with IPA®.

IPA® analysis. To determine relevant biological functions and signaling pathways of differentially expressed target-mRNAs, the target-mRNAs were uploaded into IPA® for comparative analyses (Fig. S1).

In the TIVA group, four canonical pathways were determined, all of which involved the serine/threonine protein

Table III. RNA sequencing quality and quantity.

Sequencing category	Mean library size (reads)	Mapped reads (%)	lncRNA (%)	mRNA (%)
run 1	4.11E6±1.25E6	79.70±19.32	4.61±5.05	87.47±4.84
run 2	3.54E6±9.60E5	75.38±19.87	4.81±5.01	88.25±6.86
run 3	3.43E6±6.10E5	78.60±12.01	4.54±2.38	87.72±2.63
run 4	2.76E6±5.85E5	78.10±14.33	4.18±3.89	87.51±4.66
preTIVA	3.22E6±8.83E5	73.46±18.82	4.06±2.93	86.89±3.90
postTIVA	3.85E6±8.31E5	81.77±14.03	4.74±3.08	88.81±2.26
preVAG	3.08E6±1.10E6	70.65±26.92	4.66±4.71	86.28±5.74
postVAG	3.27E6±9.75E5	81.05±20.04	4.69±6.23	88.14±8.04

lncRNA, long non-coding RNA; TIVA, total intravenous anesthesia; VAG, volatile anesthetic gas; PreTIVA, preoperative time point of TIVA; preVAG means preoperative time point of VAG; postTIVA, postoperative time point after termination of surgery during wound closure for TIVA; postVAG, postoperative time point after termination of surgery during wound closure for VAG.

kinase, homeodomain interacting protein kinase 2 (HIPK2), which is upregulated by the lncRNA FAM157A.

For the VAG-group, IPA analysis revealed eleven signaling pathways. In seven pathways the anti-apoptotic protein BCL2, downregulated by lncRNA CCDC26, were predicted to be involved. In the four other pathways, sialophorin (SPN; CD43), a highly glycosylated transmembrane protein, purinergic receptor P2X 7 (P2RX7), a purine receptor for ATP, and aldehyde dehydrogenase 5 family member A1 (ALDH5A1), a succinate semialdehyde dehydrogenase, all target-mRNAs of HELLPAR, were involved.

Additionally, target-mRNAs were also categorized to related diseases and biofunctions. The target-mRNAs of VAG demonstrated a predicted downregulation in 'Cell movement of leukocytes', 'Activation of cells' and 'Migration of cells'. For 'Neoplasia of cells' an upregulation was predicted. For TIVA, no change was predicted (Fig. 3).

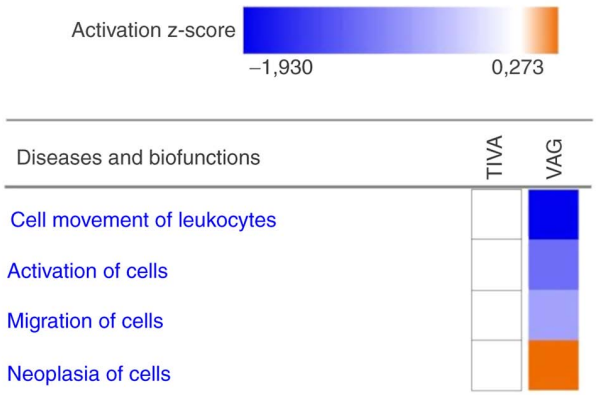

Figure 3. Effects of TIVA and VAG on tumor-related biological functions. Lower z-scores (blue) represent predicted downregulation, positive z-scores (orange) represent predicted upregulation of the pathway, indicating that no regulation could be observed. TIVA, total intravenous anesthesia; VAG, volatile anesthetic gas.

Technical validation. The regulation of selected lncRNAs and mRNAs were validated by using RT-qPCR. The results of the RT-qPCR were compared with the corresponding results of the RNA sequencing (Table V). In contrast to mRNA assays, assays for lncRNAs have not yet been well established. Nevertheless, the results for FAM157A and ST20-AS1 were obtained that confirmed the previous results. For HELLPAR, CCDC26 and TSIX, although different assays have been used (Bio-Rad Laboratories, Inc. and Qiagen, Inc.), no results could be obtained.

Discussion

The primary aim of the present proof-of-concept study was to analyze possible anesthesia-induced lncRNA and mRNA expression changes in blood. Furthermore, a main focus of the present study was to decipher the potential role of lncRNAs and their target-mRNAs as molecular players in the observed beneficial effect of TIVA on cancer outcome. In a previously performed study by the authors, anesthesia-specific miRNA expression changes were detected in circulating extracellular vesicles of CRC patients undergoing tumor resection (19). The present study extended earlier observations by the authors and concentrated on lncRNAs derived from blood, since lncRNAs represent a highly cancer-related class of non-coding RNAs (57). Blood samples obtained prior to the induction of anesthesia and following the wound closure of patients receiving either TIVA or VAG were compared and a comprehensive lncRNA and mRNA expression profiling analysis was performed. Overall, 35 differentially regulated lncRNAs for the TIVA-group and 25 for the VAG-group were identified (Table IV). With the exclusion of one lncRNA in the VAG-group, all were upregulated. These results demonstrated that lncRNA expression changes can be specific for the anesthetic regime. In addition, 1,595 differentially regulated mRNAs in the TIVA- and 947 in the VAG-intra-group comparison were detected, of which 1047 mRNAs (TIVA) and 399 mRNAs (VAG) were anesthetic-specific (Table SII).

Several lncRNAs from Table IV had already been shown to be associated with tumor growth (41,43-46), cancer cell proliferation, migration and invasion (58-61). However, the majority of lncRNAs identified in the present study have not been previously investigated. Thus far, a limited amount of research data linking lncRNAs from blood and type of

Table IV. lncRNAs regulated postoperatively compared with preoperative time point.

Regulation	lncRNA (Refs.)	baseMean	log_2FC	padj
TIVA upregulated	RP6-159A1.4	3882.13	-1.73	2.76E-06
	MIR646HG	313.00	-1.54	6.02E-04
	LINC00694	241.00	-1.77	8.83E-04
	ST3GAL4-AS1	201.26	-1.48	3.15E-03
	LINC00937	161.64	-1.53	2.13E-04
	CTB-131B5.2	144.24	-2.19	2.36E-04
	PLBD1-AS1 (40)	123.81	-1.18	2.64E-02
	AC091878.1	68.23	-1.31	3.81E-02
	FAM157C	1792.54	-1.25	2.04E-03
	FAM157A	1274.90	-1.00	1.39E-02
	TTN-AS1 (41-43)	434.98	-1.03	2.05E-03
	FAM157B	432.07	-1.39	1.44E-03
	RP11-81A1.6	422.04	-1.18	1.92E-04
	LINC01001 (44)	360.38	-1.22	1.39E-02
	RP11-83A24.2	280.34	-1.02	5.03E-03
	RP11-563J2.2	271.15	-1.54	7.84E-05
	RP4-669L17.10	269.11	-1.02	3.92E-03
	AC138035.2	129.84	-1.14	4.87E-04
	RP3-368A4.6	120.61	-1.16	1.46E-02
	LINC00211	119.63	-1.45	4.93E-08
	AC003104.1	116.80	-1.10	1.97E-02
	AC007278.2	112.79	-2.57	6.14E-06
	AC007278.3	112.72	-2.52	9.08E-07
	RP11-296O14.3	111.83	-1.05	5.20E-03
	RP11-563J2.3	104.44	-1.62	5.95E-06
	RP11-65L3.2	94.53	-1.32	5.42E-04
	CTC-490G23.2	78.78	-2.34	2.32E-04
	RP11-561P12.5	73.08	-1.41	1.92E-02
	RP11-212I21.4	72.92	-1.01	4.70E-02
	RP11-701P16.5 (45)	65.57	-1.77	3.22E-03
	CTB-31N19.3/METTL9 (46)	64.83	-1.88	2.00E-06
	RP11-981G7.1	61.78	-1.11	2.66E-02
	CTD-2530H12.2	56.48	-1.44	1.30E-03
	ST20-AS1 (47)	67.92	-1.05	5.36E-02
	RP11-242C19.2	52.96	-1.50	3.92E-03
VAG upregulated	RP6-159A1.4	2051.03	-1.42	9.55E-05
	MIR646HG	161.36	-1.45	1.46E-07
	LINC00694	129.39	-1.90	3.06E-06
	ST3GAL4-AS1	94.53	-1.70	2.75E-05
	LINC00937	82.99	-1.54	1.99E-04
	CTB-131B5.2	65.08	-2.12	4.52E-06
	PLBD1-AS1	67.11	-1.53	5.30E-05
	AC091878.1	60.44	-1.67	1.41E-03
	HELLPAR (48)	343.21	-1.23	3.26E-02
	RP11-76E17.3	156.81	-1.95	4.15E-07
	RP11-638I8.1	155.68	-1.07	1.94E-03
	RP13-580B18.4	113.59	-1.76	2.05E-03
	RP11-191L9.4	104.61	-1.67	1.28E-03
	CTA-212A2.3	82.30	-1.47	4.25E-02
	RP3-412A9.17	68.59	-1.52	4.33E-02
	CCDC26 (49-51)	57.83	-1.43	4.52E-02
	LINC00511 (52-54)	56.07	-1.50	1.52E-02

Table IV. Continued.

Regulation	lncRNA (Refs.)	baseMean	log_2FC	padj
	SNHG23 (55)	51.90	-1.97	9.79E-03
	TSIX (56)	51.72	-1.42	3.10E-02
	LINC01127 (57)	63.81	-1.07	5.85E-02
	RP11-989E6.10	82.68	-1.29	6.24E-02
	CTA-228A9.4	61.44	-1.57	7.35E-02
	RP3-394A18.1	114.24	-1.19	5.04E-02
	CH507-528H12.1	846.35	-1.13	7.58E-02
VAG downregulated	*AATBC*	58.95	1.34	5.29E-04

Filter criteria: BaseMean ≥50, |lg2FC| ≥1, padj ≤0.1. log_2FC, negative fold changes indicate the upregulation of the corresponding postoperative lncRNA, and positive fold changes display the downregulation of the corresponding lncRNA. lncRNAs specific for the anesthetic are written in italics. lncRNAs with literature reference, have already been shown to be associated with cancer (reference citations are shown in the table). lncRNA, long non-coding RNA; log_2FC, log_2 fold change; padj, adjusted P-value; baseMean, mean lncRNA expression; TIVA, total intravenous anesthesia; VAG, volatile anesthetic gas.

anesthetic used to cancer is available. As a consequence of limited data on specific lncRNAs, knowledge on their target-mRNAs and association to pathway regulations is even more scarce. To date, mainly cancer tissues or cell lines have been examined directly. For example, in human CRC cell lines, it was demonstrated that propofol promotes apoptosis, proliferation and inhibits invasion, in which the lncRNAs HOTAIR and HOXA11-AS were largely involved (62,63). However, these lncRNAs, which have already been frequently associated with cancer, could not be confirmed in the present study. Instead, the combined sequencing and *in silico* analyses of the present study revealed an association of the lncRNA FAM157A (via target-mRNA HIPK2) for the TIVA group, respectively of the lncRNAs CCDC26 (via target-mRNA BCL2) and HELLPAR (via target-mRNA SPN and P2RX7) for the VAG group with cancer-related pathways. Concerning FAM157A the analyses of the present study provided novel evidence for an association of this lncRNA and its identified target HIPK2 to several pivotal cancer signaling pathways including 'p53 Signaling', 'Cell Cycle: G2/M DNA damage checkpoint regulation', 'Molecular Mechanisms of Cancer' and the 'Senescence Pathway'. These canonical pathways were sourced from the *Knowledge Base* item underlying the IPA® software and used for the causal analytic tools 'Mechanistic Networks', 'Causal Network Analysis' and 'Downstream Effects Analysis' implemented in the software (64). The IPA *Knowledge Base* is created by millions of manually curated data obtained from scientific journals, publicly available molecular content databases, textbooks and more and allows the query, visualization and computation across the *Knowlegde Base* in relationship to miRNA and mRNA findings entered into IPA®. Previous *in vitro* and *in vivo* studies suggested that HIPK2 is a potential tumor suppressor and DNA damage-responsive kinase that activates the apoptotic program in a phosphorylation-dependent manner by targeting different downstream targets (65-67). Upregulated HIPK2 has been demonstrated to interact with the tumor suppressor p53, leading to cell cycle arrest of cancer cells during surgery (68). The results of the present study not only corroborate the effect of HIPK2 on the tumor suppressor protein p53, but also give further insight on HIPK2 upstream regulatory mechanism and a possible explanation for the anti-tumor effect of TIVA.

Another finding that emerged from the analyses is the importance of the lncRNA HELLPAR that is upregulated after VAG anesthesia. From a CRC study comparing patients with or without metastases, it is known that HELLPAR is involved in the regulation of proliferation and invasive ability of tumor cells, with higher expression in patients with metastases than without (47).

In the *in silico* analyses of the present study, it was demonstrated that HELLPAR regulates 20 out of 25 target-mRNAs in different directions. Two of these target-mRNAs, SPN (CD43) and P2RX7 (P2X7), both downregulated, were included in the 'B-Cell Development'-signaling pathway and the 'inflammasome pathway' derived from the aforementioned IPA *Knowledge Base* in colon carcinoma cells. Anti-adhesive function of SPN (CD43) expression has been associated with inhibition of adhesion to the extracellular matrix, which has implications for tumorigenesis and metastasis of CRC cells (69). The upregulation of HELLPAR with the resulting downregulation of CD43 may therefore lead to an increased adhesion of cancer cells and thus to increased metastasis. High P2RX7 expression correlated with tumor size, metastasis and poor overall survival (70). The downregulation observed in the present study could indicate a protective effect.

Another interesting finding was the association of lncRNA CCDC26 upregulation with its downregulated target-mRNA BCL2 involved in the IPA *Knowledge Base* canonical pathways 'p53 signaling', 'Autophagy', 'Interferon Signaling', 'Neuroinflammation Signaling Pathway', 'Cytotoxic T lymphocyte-mediated apoptosis of target cells', 'Docosahexaenoic Acid (DHA) Signaling' and 'Myc Mediated Apoptosis Signaling'. Decreased overall survival as well as tumor growth and apoptosis have already been linked to high CCDC26 expression (50,71). In pancreatic cancer cell cultures, CCDC26 knockdown decreased BCL2 mRNA and protein

Table V. Target-mRNAs identified *in silico* and verified in the DGE of the intra-group comparison.

		Target mRNA			
Group	lncRNA	mRNA	baseMean	log_2FC	padj
TIVA	FAM157A	*HIPK2*	789.76	-0.78	4.21E-02
	ST20-AS1	BCL9L	249.43	0.80	5.85E-02
VAG	CCDC26	*BCL2*	136.61	1.15	1.10E-06
	TSIX	TYW5	64.77	-1.01	8.06E-04
		PHACTR2	133.80	-0.56	2.51E-02
	HELLPAR	TMEM170B	199.91	-0.67	2.57E-02
		SSBP2	72.63	0.67	8.54E-02
		SPN (CD43)	190.04	0.67	2.44E-02
		SPATA13	443.65	-0.62	6.28E-02
		SLC46A3	53.37	-0.69	5.91E-02
		RNF165	54.38	-0.96	5.25E-02
		P2RX7 (P2X7)	52.66	0.81	4.69E-02
		MUC4	105.31	-1.65	3.31E-02
		MDFIC	73.85	0.71	5.31E-02
		KLRD1	243.76	-0.94	8.29E-02
		GPR27	151.79	-1.14	9.44E-08
		EXOC6	166.52	-0.88	7.74E-03
		EVL	303.50	0.87	5.84E-02
		DGKH	95.39	-1.02	7.76E-03
		CTSC	248.17	0.89	2.57E-04
		BEST1	377.61	-0.59	7.12E-02
		AUTS2	101.90	-0.85	6.26E-02
		ASPH	364.13	-1.52	1.34E-05
		ALDH5A1	110.39	0.60	6.15E-02
		AACS	60.32	-1.17	3.74E-02

Filter criteria: baseMean ≥50, $|log_2FC|$ ≥0.5, padj ≤0.1. log_2FC: Negative fold changes indicate the upregulation of the corresponding postoperative mRNA, positive fold changes show downregulation of the corresponding mRNA. mRNAs that yielded cancer-relevant results in the IPA analysis are depicted in italics. DGE, differential gene expression; lncRNA, long non-coding RNA; baseMean, mean mRNA expression; log_2FC, log_2 fold change; padj, adjusted P-value; baseMean, mean lncRNA expression; TIVA, total intravenous anesthesia; VAG, volatile anesthetic gas.

levels, while in cancer tissue CCDC26 and BCL2 were upregulated (72). Downregulation of the anti-apoptotic BCL2 ensures apoptosis in the mitochondria via release of cytochrome c and also in the nucleus, via the p53 signaling pathway (72-75). This could be explained by the VAG-induced conversion of the positive correlation between CCDC26 and BCL2 into negative correlation, thus exerting a protective effect.

An interesting conclusion derived from the results of the present study based on the mRNA data from Table V is that by using the abovementioned IPA® *Knowlegde Base* tool for interpretation of these transcription data, remarkable inhibitory effects were identified on the causal networks 'cell movement of leukocytes', 'activation of cells' and 'migration of cells' in the patients' group anesthetized by VAG. These signaling networks are crucial for the effectiveness of immune cells against tumor cells and metastasis. Constraining these cellular actions culminated in a downgraded immunological response against cancer cells. The importance of an intact immune response for tumor elimination has been proven by numerous studies (76-78).

Limitations of the present study are the relatively small sample size and that the results are not complemented by functional studies but were created by a combined sequencing and *in silico* analysis of observational data. In addition, the lncRNA and mRNA profile data are based on whole blood samples, with the profile changes deriving from the white cell fraction which is hypothesized by the authors that may be the blood fraction primarily involved in fighting cancer. It is therefore very likely that the anesthetic-related lncRNA response observed in the present study may reflect a global host response, which could in turn have effects on tumor outcome. These findings could provide evidence of a novel lncRNA mediated mechanism of anesthetic effect on immunologic and inflammatory signaling. However, an exact delineation of the relationship between anesthetic action, the immune system and cancer was not the primary aim of the present study. Drawing blood after surgery termination before wound closure was chosen as second time point, in order to ensure a sufficiently long-time interval for possible anesthesia-induced effects on intracellular RNA

expression. Certainly, it should be subsequently hypothesized that the consequences of including RNA expression changes that might be induced by the surgical procedure, at least partly, or by stress response. However, this type of confounding effects may affect both patient groups. Further limiting factors that may have an impact on the results are demographic and clinical differences present in the two cohorts. For elderly patients and patients with serious comorbidities, VAG was the choice of anesthetic in the present study. Thus, an age difference between the two groups with a P=0.016 was present and was hardly avoidable. Concerning UICC stages, stage 4 was present in two patients of the VAG group and none in the TIVA group. The influence of tumor stage on lncRNA profile is, however, beyond the scope of this pilot study and should be considered for larger cohort future studies.

In summary, the results of the present study demonstrated that general anesthesia is able to orchestrate lncRNA expression in blood, with differential and specific effects of the anesthetic agent. The analyses identified target-mRNAs for more than 17.1% (TIVA) and 28.0% (VAG) of these lncRNAs and classified them in the context of cancer-relevant signaling pathways. Canonical pathways identified for TIVA were cancer-specific and suggestive of anti-tumor effects, whereas the possible influence of VAG on tumor progression was less clear. The analysis of target-mRNA of VAG revealed a markedly worsened immunological response against cancer. These results provided preliminary evidence for the presence of a novel lncRNA-mediated mechanism of anesthetic action that, in addition to other immunoregulatory effects, may influence tumor outcome. The lncRNA results of the present study may only serve as a possible mechanistic explanation for observations in several larger cohorts in retrospective studies. Furthermore, the present study demonstrated novel effects, to the best of our knowledge, of anesthetic agents on lncRNAs with immunologic consequences not previously investigated.

According to the study design, the feasibility of detecting anesthesia specific expression changes in blood-derived lncRNA and mRNA profiles was demonstrated. Secondly, the results of the present study, which included a combined high-throughput sequencing and bioinformatic analysis, possibly indicated a non-negligible role of lncRNAs as molecular players for the proposed negative outcome of CRC patients anesthetized with VAG, in comparison to TIVA anesthetization. In addition to studies on circulating cell-free lncRNA profiles, the blood-derived lncRNA landscape may provide significant insights for different research inquiries on solid cancers and thus it appears that the further elucidation of its potential may be be a promising future study aim.

Acknowledgements

The authors would like to thank Franz Jansen, Institute of Human Genetics, University Hospital, LMU Munich for his excellent technical assistance for RT-qPCR assays.

Funding

The present study was funded by the Monika Kutzner Stiftung Grant, Rechtsfähige Stiftung des privaten Rechts zur Förderung der Krebsforschung Bayerische Straße 8, 10707 Berlin.

Availability of data and materials

All data generated in the present study may be acquired from the European Nucleotide Archive (ENA) under the accession number, PRJEB56067 (https://www.ebi.ac.uk/ena/browser/view/PRJEB56067). All other datasets used and/or analyzed during the current study are available from the corresponding author on reasonable request.

Authors' contributions

MR, GS, MWP and OKS contributed to the study conception and design. Patient recruitment, blood sampling and patient data acquisition were performed by FB, ASM and MB. Molecular analysis was performed by AL and MR. Bioinformatic analysis was performed by BK, ASM and GS. AL and MR drafted the manuscript. OKS, GS and MWP prepared the manuscript. BK and MWP confirm the authenticity of all the raw data. All authors have commented on previous versions of the manuscript and have read and approved the final manuscript.

Ethics approval and consent to participate

The Ethics Committee of the Medical Faculty of the Ludwig-Maximilians-University (LMU) Munich, Germany (to which the Institute of Human Genetics and the Department of Anesthesiology are assigned) approved the present study (protocol-no. 232-16). The present study was performed in accordance with the Declaration of Helsinki. Written informed consent was obtained and study samples were pseudonymized.

Patient consent for publication

Not applicable.

Competing interests

The authors declare that they have no competing interests.

References

1. Araghi M, Soerjomataram I, Jenkins M, Brierley J, Morris E, Bray F and Arnold M: Global trends in colorectal cancer mortality: Projections to the year 2035. Int J Cancer 144: 2992-3000, 2019.
2. Werner J and Heinemann V: Standards and challenges of care for colorectal cancer today. Visc Med 32: 156-157, 2016.
3. Demicheli R, Retsky MW, Hrushesky WJ, Baum M and Gukas ID: The effects of surgery on tumor growth: A century of investigations. Ann Oncol 19: 1821-1828, 2008.
4. Tohme S, Simmons RL and Tsung A: Surgery for cancer: A trigger for metastases. Cancer Res 77: 1548-1552, 2017.
5. Jin Z, Li R, Liu J and Lin J: Long-term prognosis after cancer surgery with inhalational anesthesia and total intravenous anesthesia: A systematic review and meta-analysis. Int J Physiol Pathophysiol Pharmacol 11: 83-94, 2019.
6. Makito K, Matsui H, Fushimi K and Yasunaga H: Volatile versus total intravenous anesthesia for cancer prognosis in patients having digestive cancer surgery. Anesthesiology 133: 764-773, 2020.

7. Guerrero Orriach JL, Raigon Ponferrada A, Malo Manso A, Herrera Imbroda B, Escalona Belmonte JJ, Ramirez Aliaga M, Ramirez Fernandez A, Diaz Crespo J, Soriano Perez AM, Fontaneda Heredia A, *et al*: Anesthesia in combination with propofol increases disease-free survival in bladder cancer patients who undergo radical tumor cystectomy as compared to inhalational anesthetics and opiate-based analgesia. Oncology 98: 161-167, 2020.
8. Jun IJ, Jo JY, Kim JI, Chin JH, Kim WJ, Kim HR, Lee EH and Choi IC: Impact of anesthetic agents on overall and recurrence-free survival in patients undergoing esophageal cancer surgery: A retrospective observational study. Sci Rep 7: 14020, 2017.
9. Zheng X, Wang Y, Dong L, Zhao S, Wang L, Chen H, Xu Y and Wang G: Effects of propofol-based total intravenous anesthesia on gastric cancer: A retrospective study. Onco Targets Ther 11: 1141-1148, 2018.
10. Wu ZF, Lee MS, Wong CS, Lu CH, Huang YS, Lin KT, Lou YS, Lin C, Chang YC and Lai HC: Propofol-based total intravenous anesthesia is associated with better survival than desflurane anesthesia in colon cancer surgery. Anesthesiology 129: 932-941, 2018.
11. Zhang T, Fan Y, Liu K and Wang Y: Effects of different general anaesthetic techniques on immune responses in patients undergoing surgery for tongue cancer. Anaesth Intensive Care 42: 220-227, 2014.
12. Yan T, Zhang GH, Wang BN, Sun L and Zheng H: Effects of propofol/remifentanil-based total intravenous anesthesia versus sevoflurane-based inhalational anesthesia on the release of VEGF-C and TGF-β and prognosis after breast cancer surgery: A prospective, randomized and controlled study. BMC Anesthesiol 18: 131, 2018.
13. Abel F, Giebel B and Frey UH: Agony of choice: How Anesthetics affect the composition and function of extracellular vesicles. Adv Drug Deliv Rev 175: 113813, 2021.
14. Ecimovic P, McHugh B, Murray D, Doran P and Buggy DJ: Effects of sevoflurane on breast cancer cell function in vitro. Anticancer Res 33: 4255-4260, 2013.
15. Iwasaki M, Zhao H, Jaffer T, Unwith S, Benzonana L, Lian Q, Sakamoto A and Ma D: Volatile anaesthetics enhance the metastasis related cellular signalling including CXCR2 of ovarian cancer cells. Oncotarget 7: 26042-26056, 2016.
16. Kvolik S, Glavas-Obrovac L, Bares V and Karner I: Effects of inhalation anesthetics halothane, sevoflurane, and isoflurane on human cell lines. Life Sci 77: 2369-2383, 2005.
17. Müller-Edenborn B, Roth-Z'graggen B, Bartnicka K, Borgeat A, Hoos A, Borsig L and Beck-Schimmer B: Volatile anesthetics reduce invasion of colorectal cancer cells through down-regulation of matrix metalloproteinase-9. Anesthesiology 117: 293-301, 2012.
18. Forrest ME, Saiakhova A, Beard L, Buchner DA, Scacheri PC, LaFramboise T, Markowitz S and Khalil AM: Colon cancer-upregulated long non-coding RNA lincDUSP Regulates cell cycle genes and potentiates resistance to apoptosis. Sci Rep 8: 7324, 2018.
19. Buschmann D, Brandes F, Lindemann A, Maerte M, Ganschow P, Chouker A, Schelling G, Pfaffl MW and Reithmair M: Propofol and sevoflurane differentially impact MicroRNAs in circulating extracellular vesicles during colorectal cancer resection: A pilot study. Anesthesiology 132: 107-120, 2020.
20. Dinger ME, Pang KC, Mercer TR and Mattick JS: Differentiating protein-coding and noncoding RNA: Challenges and ambiguities. PLoS Comput Biol 4: e1000176, 2008.
21. Bánfai B, Jia H, Khatun J, Wood E, Risk B, Gundling WE Jr, Kundaje A, Gunawardena HP, Yu Y, Xie L, *et al*: Long noncoding RNAs are rarely translated in two human cell lines. Genome Res 22: 1646-1657, 2012.
22. Guttman M, Amit I, Garber M, French C, Lin MF, Feldser D, Huarte M, Zuk O, Carey BW, Cassady JP, *et al*: Chromatin signature reveals over a thousand highly conserved large non-coding RNAs in mammals. Nature 458: 223-227, 2009.
23. Ponting CP, Oliver PL and Reik W: Evolution and functions of long noncoding RNAs. Cell 136: 629-641, 2009.
24. Gupta RA, Shah N, Wang KC, Kim J, Horlings HM, Wong DJ, Tsai MC, Hung T, Argani P, Rinn JL, *et al*: Long non-coding RNA HOTAIR reprograms chromatin state to promote cancer metastasis. Nature 464: 1071-1076, 2010.
25. Ji Q, Zhang L, Liu X, Zhou L, Wang W, Han Z, Sui H, Tang Y, Wang Y, Liu N, *et al*: Long non-coding RNA MALAT1 promotes tumour growth and metastasis in colorectal cancer through binding to SFPQ and releasing oncogene PTBP2 from SFPQ/PTBP2 complex. Br J Cancer 111: 736-748, 2014.
26. Siddiqui H, Al-Ghafari A, Choudhry H and Al Doghaither H: Roles of long non-coding RNAs in colorectal cancer tumorigenesis: A review. Mol Clin Oncol 11: 167-172, 2019.
27. Thiele JA, Hosek P, Kralovcova E, Ostasov P, Liska V, Bruha J, Vycital O, Rosendorf J, Opattova A, Horak J, *et al*: lncRNAs in Non-Malignant tissue have prognostic value in colorectal cancer. Int J Mol Sci 19: 2672, 2018.
28. Martin M: Cutadapt removes adapter sequences from high-throughput sequencing reads. EMBnet. J 17: 10-12, 2011.
29. Dobin A, Davis CA, Schlesinger F, Drenkow J, Zaleski C, Jha S, Batut P, Chaisson M and Gingeras TR: STAR: Ultrafast universal RNA-seq aligner. Bioinformatics 29: 15-21, 2013.
30. Li B and Dewey CN: RSEM: Accurate transcript quantification from RNA-Seq data with or without a reference genome. BMC Bioinformatics 12: 323, 2011.
31. Love MI, Huber W and Anders S: Moderated estimation of fold change and dispersion for RNA-seq data with DESeq2. Genome Biol 15: 550, 2014.
32. Lin Y, Liu T, Cui T, Wang Z, Zhang Y, Tan P, Huang Y, Yu J and Wang D: RNAInter in 2020: RNA interactome repository with increased coverage and annotation. Nucleic Acids Res 48 (D1): D189-D197, 2020.
33. Yang C, Yang L, Zhou M, Xie H, Zhang C, Wang MD and Zhu H: LncADeep: An ab initio lncRNA identification and functional annotation tool based on deep learning. Bioinformatics 34: 3825-3834, 2018.
34. Kanehisa M and Sato Y: KEGG Mapper for inferring cellular functions from protein sequences. Protein Sci 29: 28-35, 2020.
35. Vandesompele J, De Preter K, Pattyn F, Poppe B, Van Roy N, De Paepe A and Speleman F: Accurate normalization of real-time quantitative RT-PCR data by geometric averaging of multiple internal control genes. Genome Biol 3: RESEARCH0034, 2002.
36. Andersen CL, Jensen JL and Ørntoft TF: Normalization of real-time quantitative reverse transcription-PCR data: A model-based variance estimation approach to identify genes suited for normalization, applied to bladder and colon cancer data sets. Cancer Res 64: 5245-5250, 2004.
37. Perkins JR, Dawes JM, McMahon SB, Bennett DL, Orengo C and Kohl M: ReadqPCR and NormqPCR: R packages for the reading, quality checking and normalisation of RT-qPCR quantification cycle (Cq) data. BMC Genomics 13: 296, 2012.
38. Livak KJ and Schmittgen TD: Analysis of relative gene expression data using real-time quantitative PCR and the 2(-Delta Delta C(T)) Method. Methods 25: 402-408, 2001.
39. Deng X, Bi Q, Chen S, Chen X, Li S, Zhong Z, Guo W, Li X, Deng Y and Yang Y: Identification of a Five-Autophagy-Related-lncRNA signature as a novel prognostic biomarker for hepatocellular carcinoma. Front Mol Biosci 7: 611626, 2021.
40. Lin C, Zhang S, Wang Y, Wang Y, Nice E, Guo C, Zhang E, Yu L, Li M, Liu C, *et al*: Functional role of a novel long noncoding RNA TTN-AS1 in esophageal squamous cell carcinoma progression and metastasis. Clin Cancer Res 24: 486-498, 2018.
41. Wang Y, Li D, Lu J, Chen L, Zhang S, Qi W, Li W and Xu H: Long noncoding RNA TTN-AS1 facilitates tumorigenesis and metastasis by maintaining TTN expression in skin cutaneous melanoma. Cell Death Dis 11: 664, 2020.
42. Jia Y, Duan Y, Liu T, Wang X, Lv W, Wang M, Wang J and Liu L: LncRNA TTN-AS1 promotes migration, invasion, and epithelial mesenchymal transition of lung adenocarcinoma via sponging miR-142-5p to regulate CDK5. Cell Death Dis 10: 573, 2019.
43. Hong MEI, Changen LI, Liang Y and Yingfei GAO: Expression of lncRNA LINC01001 in breast cancer and its effect on proliferation of MCF-7 cells. Chin J Cancer Biother 25: 158-162, 2018.
44. Zhou M, Guo M, He D, Wang X, Cui Y, Yang H, Hao D and Sun J: A potential signature of eight long non-coding RNAs predicts survival in patients with non-small cell lung cancer. J Transl Med 13: 231, 2015.
45. Lv M, Cao D, Zhang L, Hu C, Li S, Zhang P, Zhu L, Yi X, Li C, Yan A, *et al*: METTL9 regulates N1-histidine methylation of zinc transporters to promote tumor growth. bioRxiv: 2021.2004.2020.440582, 2021.
46. Wang W, Zhao Z, Yang F, Wang H, Wu F, Liang T, Yan X, Li J, Lan Q, Wang J and Zhao J: An immune-related lncRNA signature for patients with anaplastic gliomas. J Neurooncol 136: 263-271, 2018.
47. Kutilin DS, Gusareva MA, Kosheleva NG, Zinkovich MS, Gvaramiya AK, Gappoeva MA, Fatkina NB, Krokhmal JN, Vasilieva EO, Karnauhova EA, *et al*: Differential expression of long noncoding RNAs in patients with metastatic and nonmetastatic colorectal cancer. J Clin Oncol 39 (15_suppl): e15023, 2021.

48. Gourvest M, Brousset P and Bousquet M: Long noncoding RNAs in acute myeloid leukemia: Functional characterization and clinical relevance. Cancers (Basel) 11: 1638, 2019.
49. Chen C, Wang P, Mo W, Zhang Y, Zhou W, Deng T, Zhou M, Chen X, Wang S and Wang C: lncRNA-CCDC26, as a novel biomarker, predicts prognosis in acute myeloid leukemia. Oncol Lett 18: 2203-2211, 2019.
50. Ma X, Li Y, Song Y and Xu G: Long Noncoding RNA CCDC26 promotes thyroid cancer malignant progression via miR-422a/EZH2/Sirt6 Axis. Onco Targets Ther 14: 3083-3094, 2021.
51. Hu Y, Zhang Y, Ding M and Xu R: LncRNA LINC00511 Acts as an oncogene in colorectal cancer via sponging miR-29c-3p to upregulate NFIA. Onco Targets Ther 13: 13413-13424, 2021.
52. Zhang J, Sui S, Wu H, Zhang J, Zhang X, Xu S and Pang D: The transcriptional landscape of lncRNAs reveals the oncogenic function of LINC00511 in ER-negative breast cancer. Cell Death Dis 10: 599, 2019.
53. Lu G, Li Y, Ma Y, Lu J, Chen Y, Jiang Q, Qin Q, Zhao L, Huang Q, Luo Z, *et al*: Long noncoding RNA LINC00511 contributes to breast cancer tumourigenesis and stemness by inducing the miR-185-3p/E2F1/Nanog axis. J Exp Clin Cancer Res 37: 289, 2018.
54. Terashima M, Ishimura A, Wanna-Udom S and Suzuki T: MEG8 long noncoding RNA contributes to epigenetic progression of the epithelial-mesenchymal transition of lung and pancreatic cancer cells. J Biol Chem 293: 18016-18030, 2018.
55. Salama EA, Adbeltawab RE and El Tayebi HM: XIST and TSIX: Novel cancer immune biomarkers in PD-L1-Overexpressing breast cancer patients. Front Oncol 9: 1459, 2020.
56. Jing L, Gong M, Lu X, Jiang Y, Li H and Cheng W: LINC01127 promotes the development of ovarian tumors by regulating the cell cycle. Am J Transl Res 11: 406-417, 2019.
57. Fang Y and Fullwood MJ: Roles, functions, and mechanisms of long Non-coding RNAs in cancer. Genomics Proteomics Bioinformatics 14: 42-54, 2016.
58. Feng H, Zhang X, Lai W and Wang J: Long non-coding RNA SLC16A1-AS1: Its multiple tumorigenesis features and regulatory role in cell cycle in oral squamous cell carcinoma. Cell Cycle 19: 1641-1653, 2020.
59. Li F, Li Q and Wu X: Construction and analysis for differentially expressed long non-coding RNAs and MicroRNAs mediated competing endogenous RNA network in colon cancer. PLoS One 13: e0192494, 2018.
60. Zhao X, Fan Y, Lu C, Li H, Zhou N, Sun G and Fan H: PCAT1 is a poor prognostic factor in endometrial carcinoma and associated with cancer cell proliferation, migration and invasion. Bosn J Basic Med Sci 19: 274-281, 2019.
61. Zhang Q, Ding Z, Wan L, Tong W, Mao J, Li L, Hu J, Yang M, Liu B and Qian X: Comprehensive analysis of the long noncoding RNA expression profile and construction of the lncRNA-mRNA co-expression network in colorectal cancer. Cancer Biol Ther 21: 157-169, 2020.
62. Zhang YF, Li CS, Zhou Y and Lu XH: Effects of propofol on colon cancer metastasis through STAT3/HOTAIR axis by activating WIF-1 and suppressing Wnt pathway. Cancer Med 9: 1842-1854, 2020.
63. Ren YL and Zhang W: Propofol promotes apoptosis of colorectal cancer cells via alleviating the suppression of lncRNA HOXA11-AS on miRNA let-7i. Biochem Cell Biol 98: 90-98, 2020.
64. Krämer A, Green J, Pollard J Jr and Tugendreich S: Causal analysis approaches in ingenuity pathway analysis. Bioinformatics 30: 523-530, 2014.
65. Sombroek D and Hofmann TG: How cells switch HIPK2 on and off. Cell Death Differ 16: 187-194, 2009.
66. Hofmann TG, Möller A, Sirma H, Zentgraf H, Taya Y, Dröge W, Will H and Schmitz ML: Regulation of p53 activity by its interaction with homeodomain-interacting protein kinase-2. Nat Cell Biol 4: 1-10, 2002.
67. Ozaki T and Nakagawara A: Role of p53 in cell death and human cancers. Cancers (Basel) 3: 994-1013, 2011.
68. Puca R, Nardinocchi L, Givol D and D'Orazi G: Regulation of p53 activity by HIPK2: Molecular mechanisms and therapeutical implications in human cancer cells. Oncogene 29: 4378-4387, 2010.
69. Park WS, Kim HJ, Lee GK, Son HS and Bae Y: Anti-adhesive functions of CD43 expressed on colon carcinoma cells through the modulation of integrins. Exp Mol Pathol 92: 82-89, 2012.
70. Lara R, Adinolfi E, Harwood CA, Philpott M, Barden JA, Di Virgilio F and McNulty S: P2X7 in cancer: From molecular mechanisms to therapeutics. Front Pharmacol 11: 793, 2020.
71. Hirano T, Yoshikawa R, Harada H, Harada Y, Ishida A and Yamazaki T: Long noncoding RNA, CCDC26, controls myeloid leukemia cell growth through regulation of KIT expression. Mol Cancer 14: 90, 2015.
72. Peng W and Jiang A: Long noncoding RNA CCDC26 as a potential predictor biomarker contributes to tumorigenesis in pancreatic cancer. Biomed Pharmacother 83: 712-717, 2016.
73. Hardwick JM and Soane L: Multiple functions of BCL-2 family proteins. Cold Spring Harb Perspect Biol 5: a008722, 2013.
74. Tsujimoto Y: Role of Bcl-2 family proteins in apoptosis: Apoptosomes or mitochondria? Genes Cells 3: 697-707, 1998.
75. Chiou SK, Rao L and White E: Bcl-2 blocks p53-dependent apoptosis. Mol Cell Biol 14: 2556-2563, 1994.
76. Blagih J, Buck MD and Vousden KH: p53, cancer and the immune response. J Cell Sci 133: jcs237453, 2020.
77. Bronte V, Cingarlini S, Marigo I, De Santo C, Gallina G, Dolcetti L, Ugel S, Peranzoni E, Mandruzzato S and Zanovello P: Leukocyte infiltration in cancer creates an unfavorable environment for antitumor immune responses: A novel target for therapeutic intervention. Immunol Invest 35: 327-357, 2006.
78. Garziera M and Toffoli G: Inhibition of host immune response in colorectal cancer: Human leukocyte antigen-G and beyond. World J Gastroenterol 20: 3778-3794, 2014.
79. Brierley JD, Gospodarowicz MK, Wittekind C (eds): TNM Classification of Malignant Tumours. 8th Edition. Wiley-Blackwell, New Jersey, pp272, 2016